PCCP

RSC Publishing

PAPER

View Article Online
View Journal | View Issue

Cite this: *Phys. Chem. Chem. Phys.*, 2013, **15**, 16746

Electron donor ionic liquids entrapped in anionic and cationic reverse micelles. Effects of the interface on the ionic liquid–surfactant interactions†

Diana Blach, Juana J. Silber, N. Mariano Correa and R. Darío Falcone*

Received 30th May 2013,
Accepted 5th August 2013

DOI: 10.1039/c3cp52273c

www.rsc.org/pccp

The behavior of two ionic liquids (ILs) with high electron donor ability such as 1-butyl-3-methylimidazolium trifluoromethanesulfonate (bmimTfO) and 1-butyl-3-methylimidazolium trifluoroacetate (bmimTfA) entrapped in anionic and cationic reverse micelles (RMs) was investigated using dynamic light scattering (DLS) and FT-IR spectroscopy. The systems studied were chlorobenzene/sodium 1,4-bis-2-ethylhexylsulfosuccinate (AOT)/bmimTfO, chlorobenzene/AOT/bmimTfA, chlorobenzene/benzyl-*n*-hexadecyldimethylammonium chloride (BHDC)/bmimTfO and chlorobenzene/BHDC/bmimTfA. DLS results reveal the formation of RMs containing bmimTfO and bmimTfA as polar components since the droplet size values increase as W_s (W_s = [IL]/[surfactant]) increases. To the best of our knowledge this is the first report where it is shown that both ILs are entrapped by AOT and BHDC surfactants to effectively create RMs. Furthermore, it is shown that the RMs consist of discrete spherical and non-interacting droplets of IL stabilized by the surfactants. The larger droplet size values and the larger changes obtained for bmimTfO entrapped in AOT and BHDC RMs in comparison with those for bmimTfA in both RMs can be explained considering the different IL–surfactant interactions. The FT-IR results suggest that the ionic interactions (with the surfactant polar head groups, surfactant counterions or with the IL counterions) are substantially modified upon confinement. These interactions produce segregation of ILs's ions altering the composition of the RM interfaces. These facts show the versatility of this kind of organized systems to alter the ionic organization, information that can be very important if these media are used as nanoreactors because unique microenvironments can be easily created simply changing the RM components and W_s.

Introduction

Reversed micelles (RMs) are spatially ordered macromolecular assemblies of surfactants formed in non-polar solvents, in which the polar head groups of the surfactants point inward and the hydrocarbon chains point toward the non-polar medium.[1–3] There are a wide range of surfactants that form RMs, including anionic, cationic and nonionic molecules.[1–29] Probably, the anionic surfactant most frequently used to create RMs is sodium 1,4-bis-2-ethylhexylsulfosuccinate (AOT, Scheme 1).[4–6,8–10,15–17,19,22,23,25,28] The traditional solvent used as a polar component in RMs is water[4,5,7,10,14,15,17–19,22,23,25] but other non-aqueous solvents[29] are also entrapped in the polar core, forming a polar pool surrounded by a layer of surfactant molecules dispersed in the non-polar pseudophase. The cationic surfactant, benzyl-*n*-hexadecyldimethylammonium chloride (BHDC, Scheme 1), also forms RMs in aromatic solvents without addition of a cosurfactant.[5,7,10,15,17–21,26–28]

Ionic Liquids (ILs) have received significant attention as powerful alternatives to conventional molecular organic solvents.[30–32] Negligible vapor pressure combined with excellent chemical and thermal stability, ease of recyclability and widely tunable properties such as polarity, hydrophobicity and solvent miscibility through appropriate modification of the cation and the anion make ILs neoteric solvents for a number of chemical processes.[30–33] The most ILs used are based on *N*,*N*′-dialkylimidazolium cations, especially 1-butyl-3-methylimidazolium ($bmim^+$) and different anions such as tetrafluoroborate (BF_4^-), hexafluorophosphate (PF_6^-) and bis(trifluoromethylsulfonyl)imide (Tf_2N^-).

One type of attractive RM system utilized ILs as polar components (IL RMs).[26–28,34–44] These IL RMs have gained attention because of their potential applications owing to the unique features of both ILs and RMs. The most used IL in this kind of systems is $bmimBF_4$[26,27,36a,b,d,e,37c,42b,43] however, few reports about the encapsulation of $bmimPF_6$[40c] or $bmimTf_2N$[26,28] in RMs are found in the literature. The most

Departamento de Química, Universidad Nacional de Río Cuarto, Agencia Postal # 3, C.P. X5804BYA Río Cuarto, Argentina. E-mail: rfalcone@exa.unrc.edu.ar

† Electronic supplementary information (ESI) available. See DOI: 10.1039/c3cp52273c

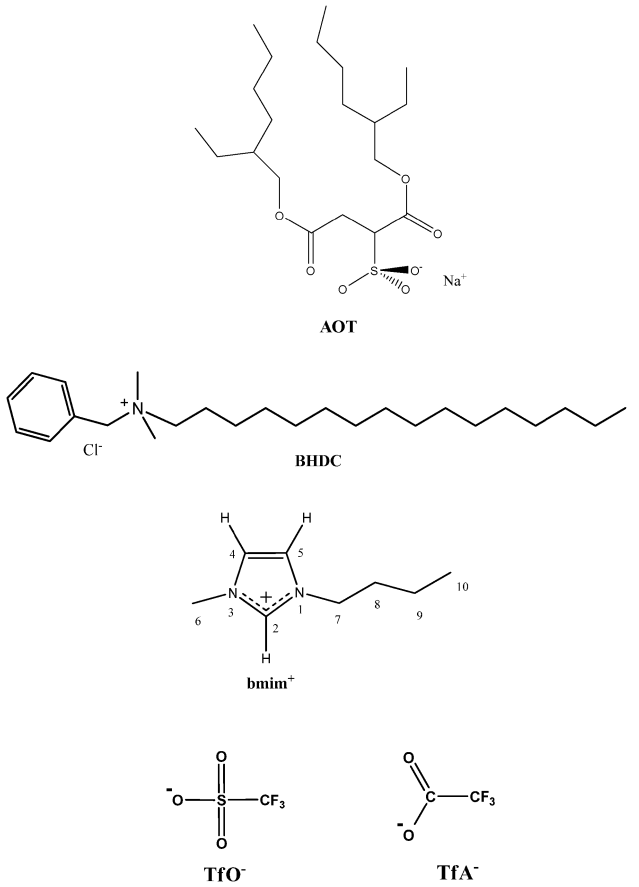

Scheme 1 Molecular structure of AOT, BHDC, $bmim^+$, TfO^- and TfA^-.

common surfactant used to create IL RMs is the nonionic Triton X-100 (TX-100).[26,27,34a–c,38,40,43] The results obtained by different authors suggest that when ILs are entrapped in TX-100 RMs, the ILs do not interact strongly with the nonionic surfactant at the interface of RMs and, in consequence their structure and properties remain quite similar in comparison with the behavior in neat IL. On the other hand, more scarce are the investigations using BHDC[26–29,42b] or AOT[28,44,45] as a surfactant and ILs such as $bmimBF_4$ or $bmimTf_2N$. Important differences in the structure of the ILs entrapped inside BHDC RMs, in comparison with the neat ILs or entrapped in TX-100 or AOT RMs, were observed from absorption, FT-IR and NMR measurements.[26–29]

As described above, the ILs commonly used in RMs are $bmimBF_4$, $bmimTf_2N$ and $bmimPF_6$ and all of them are solvents with low electron donor capacity.[46] Interesting ILs formed by anions with high electron donor ability such as trifluoromethanesulfonate[46] (TfO^- in Scheme 1) have been used as solvents to perform different S_N2 reactions in homogeneous media.[33,47] In those works, the authors showed that the solvent offers a particular environment in comparison with molecular solvents. In this way, it is well known that the physicochemical properties of polar solvent entrapped inside RMs change dramatically from the bulk solvents as a result of the specific interactions and confined geometries.[2,4–6,8–10,16,17] Moreover, it has been demonstrated that the effect of the kind of surfactant used to create RMs is crucial for the understanding of the polar solvent structure.[10,15,17] Taking this under consideration we want to explore if two different ILs formed by anions with high electron donor ability[46] such as: 1-butyl-3-methylimidazolium trifluoromethanesulfonate (bmimTfO, Scheme 1) and 1-butyl-3-methylimidazolium trifluoroacetate (bmimTfA, Scheme 1) can be used as polar solvents in order to create IL RMs. Moreover, we want to study the effect on the entrapped IL structure of the: (i) variation of the kind of interfaces (using AOT and BHDC as surfactants to create RMs) and, (ii) variation of IL content defined as W_s (W_s = [IL]/[surfactant]). To the best our knowledge there is not information about the encapsulation of bmimTfO and bmimTfA inside AOT and BHDC RMs. To monitor the formation and obtain valuable information about the molecular interactions of these novel RMs, we have chosen the DLS technique and FT-IR spectroscopy, respectively. DLS is commonly used to reveal the formation of organized systems[9,26,28,38,48] and FT-IR is essential to obtain knowledge about the microstructure of RMs.[8,28,49–54]

Experimental section

Materials

Sodium 1,4-bis (2-ethylhexyl) sulfosuccinate (AOT) from Sigma (>99% purity) and benzyl-*n*-hexadecyldimethylammonium chloride (BHDC), from Sigma (>99% purity), were used as received. Both surfactants were dried under vacuum prior to use. Chlorobenzene from Sigma (HPLC quality) was used without prior purification.

The ILs used, 1-butyl-3-methylimidazolium trifluromethanesulfonate (bmimTfO) and 1-butyl-3-methylimidazolium trifluoroacetate (bmimTfA), were synthesized under anaerobic conditions using standard Schlenk techniques.[55,56] Prior to use, both ILs were discolored with activated charcoal, filtrated through basic aluminum oxide and dried under vacuum at 60 °C for 4 hours.[57]

To simulate the interactions of 1-butyl-3-methylimidazolium ($bmim^+$) with the different anions present in the RMs ($bmim^+$–Cl^- in BHDC or $bmim^+$–SO_3^- in AOT), we synthesized 1-butyl-3-methylimidazolium chloride (bmimCl)[55,56] and, a molecule where the Na^+ counterion in the AOT was replaced by $bmim^+$ (bmimAOT), following the experimental procedure in Brown *et al.* work.[58]

Methods

The stock solutions of surfactants in chlorobenzene were prepared by mass and volumetric dilution. Aliquots of these stock solutions were used to make individual reverse micelle solutions with different amounts of IL, defined as W_s = [IL]/[surfactant]. The incorporation of IL into each micellar solutions was performed using calibrated microsyringes. To obtain optically clear solutions they were shaken in a sonicating bath. The resulting solutions were clear with a single phase and they were used in DLS experiments to determine the RM size. Similar sample preparation was used for FT-IR experiments.

W_s was varied between 0–3.0 for chlorobenzene/BHDC/bmimTfA and chlorobenzene/AOT/bmimTfA, between 0–1.5 for chlorobenzene/AOT/bmimTfO and, between 0–2.5 for chlorobenzene/BHDC/bmimTfO RMs. It was not possible to obtain higher values of W_s due to turbidity problems. The lowest value for W_s ($W_s = 0$) corresponds to a system without the IL addition. In all cases, the surfactant concentration was kept constant and equal to 0.02 M. It is important to note that bmimTfO and bmimTfA at room temperature are not soluble in chlorobenzene, and neither in chlorobenzene/AOT nor chlorobenzene/BHDC solutions at surfactant concentrations lower than the critical micelle concentration (around 10^{-3} M).[7,11–13]

General

The apparent diameters of the different IL RMs were determined by dynamic light scattering (DLS, Malvern 4700 with goniometer) using an argon-ion laser operating at 488 nm. Cleanliness of the cuvettes used for measurements was of crucial importance for obtaining reliable and reproducible data.[59] Cuvettes were washed with ethanol, and then with doubly distilled water and dried with acetone. Prior to use the samples were filtered three times using an Acrodisc with 0.2 μm PTFE membranes (Sigma) to avoid dust or particles present in the original solution. Before introducing each sample to the cuvette, it was rinsed with pure chlorobenzene twice, then with the 0.02 M surfactant stock solution, and finally with the sample to be analyzed. Prior to making measurements on a given day, the background signals from air and chlorobenzene were collected to confirm cleanliness of the cuvettes. Prior to data acquisition, samples were equilibrated in the DLS instrument for 10 min at 25 °C. To obtain valid results from DLS measurements requires knowledge of the system's refractive index and viscosity in addition to well-defined conditions. Since we worked with dilute solutions, the refractive indices and viscosities for the RM solutions were assumed to be the same as neat chlorobenzene.[60] Multiple samples at each size were made, and thirty independent size measurements were made for each individual sample at a scattering angle of 90°. The instrument was calibrated before and during the course of experiments using several different size standards. Thus, we are confident that the magnitudes obtained by DLS measurements can be taken as statistically meaningful for all the systems investigated. The algorithm used was CONTIN and the DLS experiments show that the polydispersity of the size of IL RMs is less than 5%. The droplets of IL RMs scatter very weakly at $W_s < 0.5$, and the d_{app} is below 1 nm, which is the lower particle size magnitude detectable with reliability by DLS. Consequently, $W_s = 0.5$ was selected as a measuring start point in the majority of the experiments.

The aggregation numbers (N_{agg}) of the IL RMs were determined using the static light scattering (SLS) technique in the same equipment as that used in DLS. All the measurements were made at an angle of 90° and Debye plots were created using solutions with different surfactant concentration at fixed W_s for all the RMs studied. From the SLS experiments, the weight-averaged molar masses were determined and the N_{agg} values for all the systems investigated were calculated according to the procedure detailed in the literature.[61]

FT-IR spectra were recorded using a Nicolet IMPACT 400 spectrometer. The FT-IR measurements in neat ILs (bmimTfO and bmimTfA) were taken in Irtran-2 cell of 0.015 mm path length from Wilmad Glass (Buena, NJ), while for the RM samples, Irtran-2 cell of 0.5 mm of path length was used. FT-IR spectra were obtained by co-adding 200 spectra at a resolution of 0.5 cm^{-1}. Due to that the sulfonate and carbonyl intense infrared bands[62,63] of AOT are in the same region as that of the TfO's asymmetric S=O stretching band and the TfA's asymmetric carboxylate stretching band, respectively, each FT-IR spectrum varying the W_s in both AOT RMs was obtained using a chlorobenzene/AOT solution at $W_s = 0$ as the background.[49,50] For the FT-IR performed in BHDC RMs, the chlorobenzene spectrum was used as the background.

All the experiments were carried out at 25 ± 0.5 °C.

Results and discussion

The results obtained in this work are presented in two sections. In the first part, we show the data obtained using the DLS technique and, in the second part we report the results obtained using FT-IR spectroscopy.

(1) DLS experiments

To evaluate the formation of the new RMs, the systems formed by chlorobenzene/AOT/bmimTfO, chlorobenzene/AOT/bmimTfA, chlorobenzene/BHDC/bmimTfO and chlorobenzene/BHDC/bmimTfA were studied using the DLS technique. Chlorobenzene was chosen as non-polar solvent because it is capable of forming clear and stable ternary mixtures with the ILs and surfactants investigated.

The first question that has to be answered when new reversed micellar systems are explored is if the polar solvent (IL in our case) is effectively entrapped by the surfactant creating true RMs in the non-polar solvent.[9]

In our work, as all the DLS experiments were carried out at fixed surfactant concentration (0.02 M) consequently, the RM solutions are not at infinite dilution. Thus, we think appropriate to introduce an apparent hydrodynamic diameter (d_{app}) in order to make the comparison of our systems. A similar approach was used previously.[18,64] In Fig. 1A and B, we report the d_{app} values obtained for bmimTfO and bmimTfA entrapped in the AOT and BHDC RMs studied at different W_s values, respectively. As it can be seen in both figures, there is an increase in the droplet size values when the IL content increases in all the systems, showing that both ILs are effectively entrapped by the surfactant layer yielding RMs. Moreover, the fact that the droplet size values increase with the ILs content show that the ILs are located at the interfaces of the RMs and interacting with them.[9,29] Also, the linear tendency observed in the whole W_s range for the AOT and BHDC RMs suggests that the RMs are spherical and non-interacting droplets.[2,26]

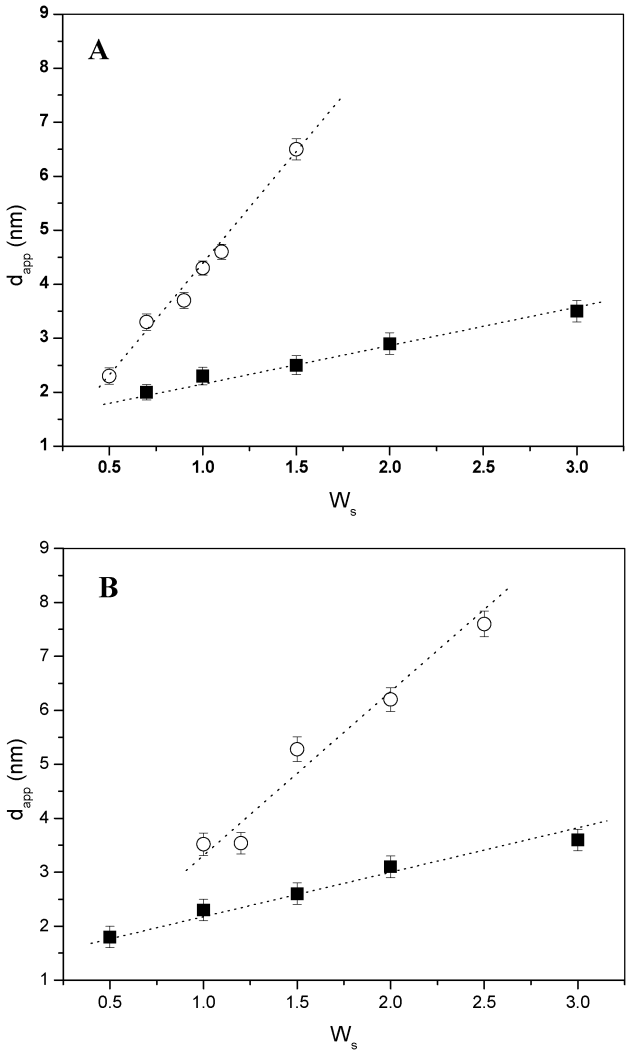

Fig. 1 Apparent diameter (d_{app}) values for (A) chlorobenzene/AOT and (B) chlorobenzene/BHDC RMs obtained at 25 °C varying W_s. (■) bmimTfA and (○) bmimTfO. [Surfactant] = 0.02 M. The straight lines were plotted to guide the eye.

As it can be seen from Fig. 1, the sizes obtained for the anionic and cationic RMs are comparable to the values reported previously[26,28] for this class of organized systems but entrapping different ILs. An interesting result is that the magnitudes of the droplet size changes are dependent on the type of IL entrapped. For example, at W_s = 1.5 the droplet size value is 2.5 nm for chlorobenzene/AOT/bmimTfA and 6.5 nm for chlorobenzene/AOT/bmimTfO (Fig. 1A). Also, in the cationic RMs it is possible to observe the similar tendency, where the RMs containing bmimTfO are the largest. Thus, in chlorobenzene/BHDC/bmimTfA the d_{app} is 2.6 nm while in chlorobenzene/BHDC/bmimTfO the value observed is 5.2 nm at W_s = 1.5 (Fig. 1B). To explain these results it is important to consider that the droplet sizes of RMs depend, among many other variables, on the effective packing parameter of the surfactants, $p = v/al_c$, in which v and l_c are the volume and the length of the hydrocarbon chain, respectively, and a is the surfactant head group area.[65] The RM sizes are larger when the surfactant packing parameter values are smaller.[66] Since the polar head group nature of both surfactants (AOT and BHDC) is completely different, the p parameters are not similar,[11,65] in consequence it is not valuable to compare the d_{app} values obtained for AOT and BHDC RMs. Therefore, we will compare the data separately for each RMs.

To explain why bmimTfO containing RMs are large in comparison with the RMs with bmimTfA we have to consider the interaction of the ILs with the interface. We have shown in non aqueous *n*-heptane/AOT RMs[9] that the polar solvents–AOT interactions are the key for the droplet size control of RMs. For example, when a polar solvent encapsulated interacts strongly (by hydrogen bonding) with the AOT polar head group, it increases the surfactants' a values with the consequent decrease in the surfactant packing parameter, and increases the RM droplet size. The same considerations have been obtained for BHDC RMs, with water[18] or ILs such as $bmimBF_4$ or $bmimTf_2N$ as the polar component.[26,28] Thus, we can assume that the larger droplet size values and the larger changes obtained for bmimTfO entrapped in AOT and BHDC RMs in comparison with the values obtained for bmimTfA can be explained considering the different IL–surfactant interactions. When bmimTfO is encapsulated in AOT RMs, the cation $bmim^+$ can penetrate the interface toward the SO_3^- group and, the anions TfO^- can interact with the Na^+ counterions. Thus, the presence of $bmim^+$ at the interface increases the effective interfacial area, decreases the surfactant packing parameter with the consequent increase in the RMs size. In contrast, the small droplet size changes observed when bmimTfA is added to the AOT RMs suggests a weak IL–AOT interaction and none of the ions ($bmim^+$ and TfA^-) are located at the interface. The question is why bmimTfO can penetrate at the interface and bmimTfA does not? The main difference between these two ILs is the higher electron donor ability of bmimTfA in comparison to bmimTfO, both having similar polarities.[67] Thus, we hypothesize that it is very likely that the interaction between $bmim^+$ and TfA^- is stronger upon confinement making stronger the ion-pair associations and showing a weak interaction toward the anionic AOT polar head. Consequently, not large changes in the packing parameter and in the droplet sizes are expected when varying the IL content. Similar results were found when molecular solvents such as dimethylformide[9] and dimethylacetamide[9] or IL such as $bmimTf_2N$[28] are encapsulated inside AOT RMs.

Similarly, comparing the d_{app} values obtained for both ILs in the BHDC RMs (Fig. 1B) suggests that the anion TfO^- interacts stronger with the positive charge of the cationic surfactant polar head group (BHD^+) than TfA^- and, consequently penetrates more the interface of RMs, increasing the effective interfacial area, decreasing the surfactant packing parameter and increasing the size of RMs. These results also suggest a large ion separation of the ionic components of bmimTfO inside the BHDC RMs, probably because a strong IL–BHD interaction. On the other hand, the small changes in the d_{app} values obtained in the chlorobenzene/BHDC/bmimTfA system

Table 1 Comparison of the droplet sizes (d_{app}) and aggregation number (N_{agg}) values obtained in different RMs. [Surfactant] = 0.1 M. T = 25 °C

System	W_s	d_{app} (nm)	N_{agg}
Chlorobenzene/AOT/bmimTfO	1	4.3 ± 0.2	40 ± 2
Chlorobenzene/AOT/bmimTfA	1	2.0 ± 0.2	28 ± 2
Chlorobenzene/BHDC/bmimTfO	1	3.3 ± 0.1	27 ± 2
Chlorobenzene/BHDC/bmimTfA	1	2.3 ± 0.2	17 ± 2

suggests a weaker TfA^-–BHD^+ interaction than the TfO^-–BHD^+, as it was observed for bmimTfA entrapped in AOT RMs. Thus, the DLS results clearly show that the cation–anion interactions present in the bulk IL structure can be modified upon confinement.

In order to obtain more valuable information about the IL RMs investigated, the SLS technique was used to determine the aggregation numbers (N_{agg}) of the systems at W_s = 1, and the values are listed in Table 1. As it can be seen, all the N_{agg} values obtained are comparable with those reported in aqueous RMs such as benzene/AOT/water[68] or chlorobenzene/BHDC/water.[69] Interestingly, the N_{agg} values are different for bmimTfO and bmimTfA RMs, for example in chlorobenzene/AOT/bmimTfO the N_{agg} value is around 40, being around 28 for chlorobenzene/AOT/bmimTfA according to the bigger size of the former system. A similar tendency is observed for both ILs entrapped in BHDC RMs (see Table 1). Moreover, as it was reported for other RMs,[2] the magnitude of the N_{agg} obtained in these systems also suggests that the shape of the RMs is practically spherical as it was assumed by DLS experiments.

(2) FT-IR experiments

In order to acquire a full panorama of these novel RMs, we choose to monitor the microenvironment that the ions $bmim^+$ and TfO^- in bmimTfO, and $bmim^+$ and TfA^- in bmimTfA sense inside AOT and BHDC RMs. Thus, the aromatic C–H stretching modes of the cation $bmim^+$ in both ILs, the asymmetric S=O stretching mode of the anion TfO^- and the asymmetric carboxylate stretching mode of the anion TfA^- were evaluated and, finally the results were compared to stretching vibration modes of the neat ILs.

(2.1) C–H stretching band (ν_{C-H}). For the ILs composed of 1-alkyl-3-methyl imidazolium, the infrared peaks found between 3200 and 3100 cm^{-1} are assigned to the aromatic C–H stretching modes of C(2)–H and C(4,5)–H on the imidazolium cation (Scheme 1).[28,70,71] The band at lower frequency is assigned to the C(2)–H stretching modes because the group has a larger positive charge density than the C(4,5)–H groups, which leads to smaller force constants.[72] Thus, the band at the higher frequencies is attributed to the C(4,5)–H stretching modes.[28,70] These stretching vibrations in $bmim^+$ can be used to evaluate the cation–anion interactions in complex systems such as RMs[28] since $bmim^+$ interacting strongly with anions can diminish its positive charge density with the consequent decrease in the ν_{C-H} values.[72]

Fig. 2 shows the FT-IR spectra of bmimTfO incorporated into chlorobenzene/AOT RMs at different W_s values, in the region of 3200–3100 cm^{-1}. The spectra obtained for

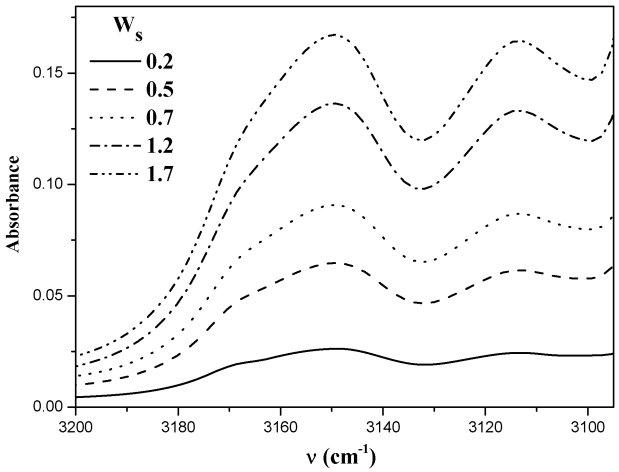

Fig. 2 FT-IR spectra of bmimTfO entrapped in chlorobenzene/AOT RMs at different W_s values, in the region of 3200–3100 cm^{-1}. [AOT] = 0.02 M. The chlorobenzene and AOT bands have been subtracted.

chlorobenzene/AOT/bmimTfA, chlorobenzene/BHDC/bmimTfO and chlorobenzene/BHDC/bmimTfA RMs are collected in Fig. S1A, B, C, respectively, in the ESI.† As it is observed from Fig. 2 and Fig. S1 (ESI†), both aromatic C–H stretching modes in the BHDC and AOT RMs can be studied. However, taking into account the proximity of the C(2)–H stretching band of $bmim^+$ and the strong aromatic C–H stretching mode of chlorobenzene (around 3080 cm^{-1}), the C(2)–H stretching band can be affected by the aromatic external solvent even subtracting chlorobenzene bands. Thus, in order to avoid wrong interpretations we only discussed the C(4,5)–H stretching band. Shifts of the C(4,5)–H stretching frequency upon increasing W_s in the different RMs are plotted in Fig. 3 for bmimTfO (3A) and for bmimTfA (3B) and they are compared with the corresponding value obtained for both neat ILs (Fig. S2, ESI†). The results show that the behavior of both ILs entrapped in BHDC and AOT RMs is clearly different. For example, at W_s = 0.25 the $\nu_{C(4,5)-H}$ appears at 3149 cm^{-1} and 3145 cm^{-1} in bmimTfO/AOT/chlorobenzene and bmimTfO/BHDC/chlorobenzene, respectively, while, in neat bmimTfO the value appears at 3154 cm^{-1} (see Fig. S2A, ESI†). When bmimTfA is the IL entrapped, at W_s = 0.25 the $\nu_{C(4,5)-H}$ appears at 3147 cm^{-1} and 3146 cm^{-1} in bmimTfA/AOT/chlorobenzene and bmimTfA/BHDC/chlorobenzene, respectively, while in neat bmimTfA the value is 3149 cm^{-1} (see Fig. S2B, ESI†). Thus, the C(4,5)–H stretching frequency values are shifted to lower frequencies when bmimTfO is entrapped in BHDC and AOT RMs in comparison with the corresponding value for neat bmimTfO. However, when bmimTfA is encapsulated in both RMs the C(4,5)–H stretching frequency values are practically the same in both RMs and are slightly shifted to lower frequencies than the value in neat bmimTfA.

The variation in the observed values of the C(4,5)–H vibration modes (Fig. 3A) between bmimTfO entrapped in AOT or BHDC RMs and neat bmimTfO is evidence of an important perturbation on the IL entrapped in both RMs. Evidently there

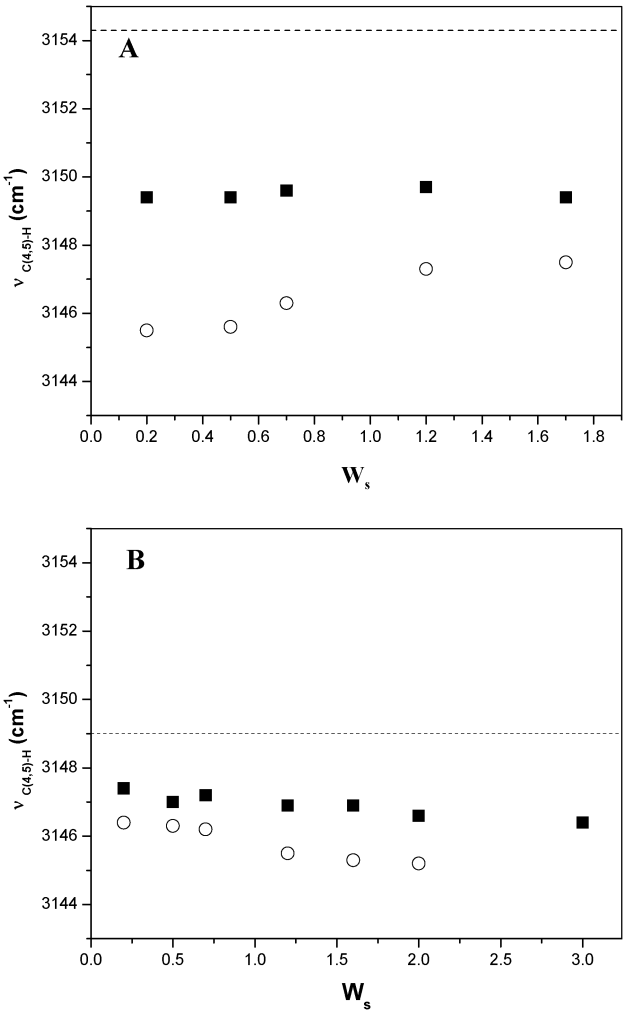

Fig. 3 Shift of the C(4,5)–H stretching frequencies of $bmim^+$ (A: bmimTfO and B: bmimTfA) upon increase of W_s in different chlorobenzene/surfactant/IL RMs: (■) AOT and (○) BHDC. [Surfactant] = 0.02 M. The corresponding value for neat IL (---) is included for comparison.

are interactions that are not present in the neat bmimTfO structure because the cation $bmim^+$ in bmimTfO shows the significant structure alteration upon encapsulation. As it was proposed from the DLS results, we think that the BHDC surfactant counterion (Cl^-) or the sulfonate in AOT exchanges with the TfO^- in entrapped bmimTfO. That is, in the AOT RMs, $bmim^+$ can be located between the AOT molecules at the interface expelling the Na^+ counterion. In BHDC RMs the TfO^- anions partition the interfacial region replacing the regular Cl^- counterion and placing the TfO^- in close proximity to the positive surfactant head group (BHD^+). Thus, we suggest that the $bmim^+$ interacting with the Cl^- counterion or SO_3^- diminishes the positive charge density over $bmim^+$ with the consequent lower ν_{C-H} frequency shifts as shown in Fig. 3A. Similar shifts are observed for the C–H stretching frequencies of the neutral imidazole molecule and the imidazolium cation, where the ν_{C-H} value for imidazole appears at a lower value than the positive imidazolium.[72] It is well known that reduction on the positive charge density over the imidazolium cation shifts the C–H frequencies to lower values.[72] Moreover, to support the idea about the interactions of $bmim^+$ with the different anions present in the RMs ($bmim^+$–Cl^- in BHDC or $bmim^+$–SO_3^- in AOT), we made additional experiments. Thus, we compared the ν_{C-H} frequency values in chlorobenzene/BHDC/bmimTfO RMs with the corresponding value obtained in neat 1-butyl-3-methylimidazolium chloride (bmimCl). The ν_{C-H} frequency value obtained for bmimCl is 3149 cm^{-1}. Additionally, to simulate the interaction between $bmim^+$ and sulfonate groups, we synthesized a molecule where the Na^+ counterion in the AOT was replaced by $bmim^+$ (bmimAOT). In this case we obtained a ν_{C-H} frequency value of 3148 cm^{-1}. As it can be seen both frequencies (in bmimAOT and in bmimCl) are lower than the value obtained for bmimTfO neat (3154 cm^{-1}), suggesting that effectively the positive charge density over $bmim^+$ diminishes as a consequence of a strong interaction with anions different to TfO^-. Moreover, as shown in Fig. 3A the values of ν_{C-H} frequency of bmimTfO entrapped in BHDC and AOT RMs are very similar to those obtained for bmimCl and bmimAOT, showing that in fact $bmim^+$ interacts with Cl^- or SO_3^-.

Furthermore, the changes in the droplet size values in the RMs containing bmimTfO (Fig. 1) also denote a particular structural organization, showing the bmimTfO penetration at the interface. Additionally, the independence of the $\nu_{C(4,5)-H}$ values with the bmimTfO content denotes that $bmim^+$ is always sensing the presence of SO_3^- in AOT or Cl^- in BHDC around it.

(2.2) TfO's asymmetric S═O stretching band ($\nu_{asym}SO_3$). The anion TfO^- is known to be highly sensitive to its state of coordination with different cations and exhibits characteristic infrared absorption bands in the vibrational spectra depending upon the typical anionic environment.[73–76] Particularly, the local environment surrounding the TfO^- anions in solution can be investigated by monitoring one vibrational mode of the TfO^- anion: the SO_3 asymmetric stretching motion, $\nu_{asym}SO_3$. The SO_3 stretching vibrations were investigated earlier using infrared spectroscopy[73–78] and the $\nu_{asym}SO_3$ stretching region was observed at 1320–1200 cm^{-1}. This SO_3 asymmetric stretching mode provides important information about the strength of cation–anion interactions. The non-coordinated (free) TfO^- ion is assumed to have the point group symmetry C_{3v}, where SO_3 asymmetric stretching mode is a doubly degenerate mode and the $\nu_{asym}SO_3$ value was observed at around 1272 cm^{-1}.[79,80] When TfO^- interacts with cations, the symmetry of the TfO^- ion is lowered, causing a splitting of the asymmetric SO_3 stretching mode into two components (around 1290 and 1255 cm^{-1}),[81] as result from the lifting of the degeneracy in the TfO^- ion.[82] The size of the splitting, defined as $\Delta\nu_{asym}SO_3$, is indicative of the strength of the perturbation of the anion by the cations, being larger when the ionic interaction is stronger.[83–85] The role of these interactions has been closely examined by parallel studies of different TfO salts in homogeneous media (protic and aprotic solvents), since the cations can exhibit quite different degrees of cation–anion interactions.[86–88] Splitting of the degenerate asymmetric SO_3 stretching mode on coordination of TfO^- to cations has been observed in many cases and a large

split is obtained if the radius of the ion is decreased, due to a strong interaction with a small cation. For example, the $\Delta\nu_{asym}SO_3$ value is 73 cm^{-1} for Mg^{2+}, 66 cm^{-1} for Ca^{2+}, 50 cm^{-1} for Sr^{2+}, and 45 cm^{-1} for Ba^{2+}.[89] Also, the charge density is important in order to evaluate the $\Delta\nu_{asym}SO_3$ changes. For example, the lithium ion has a very high charge density and is expected to strongly interact with the oxygen atoms of the SO_3 end of the TfO^- anion. In contrast, tetrabutylammonium is a large cation with a well-protected charge; consequently the cation–anion interactions are expected to be quite small. Thus, the asymmetric SO_3 stretching vibration in the lithium TfO salt was observed experimentally to split by 48 cm^{-1},[90] in contrast no lifting of the degeneracy was seen in the corresponding solutions of tetrabutylammonium TfO, and a single band at about 1271 cm^{-1} was observed. This single band was assigned to ''free'' ions considering the bulky nature of the tetrabutylammonium cation.[91] Thus, if the SO_3 group does not interact specifically with the environment, the band is fully symmetric.[92] For neat bmimTfO (see Fig. S2A, ESI†), the broad peak at 1263 cm^{-1} is attributed to the SO_3 asymmetric stretching,[93] and the absence of splitting in this band suggests a weak $bmim^+$–TfO^- interaction in neat solvent.

In Fig. 4 typical FT-IR spectra of bmimTfO inside chlorobenzene/AOT RMs at different W_s values, in the region of 1320–1200 cm^{-1} corresponding to the $\nu_{asym}SO_3$ of TfO^-, are reported. Spectra obtained for chlorobenzene/BHDC/bmimTfO RMs are presented in Fig. S3 (ESI†). From Fig. 4 and Fig. S3 (ESI†) it is possible to observe the splitting of the two intense peaks. Shifts of the $\Delta\nu_{asym}SO_3$ values upon increase of W_s in the RMs studied are shown in Fig. 5. As it can be observed, the $\Delta\nu_{asym}SO_3$ values in RMs are very different in both RMs studied. Additionally, Fig. 5 also shows that the $\Delta\nu_{asym}SO_3$ values for bmimTfO in AOT and BHDC RMs are strongly dependent on the amount of IL entrapped. For example, at W_s = 0.2 the $\Delta\nu_{asym}SO_3$ values are 32.8 cm^{-1} in AOT RMs and 19 cm^{-1} in BHDC RMs, while at W_s = 1.7, the $\Delta\nu_{asym}SO_3$ values are 18.7 cm^{-1} and 15 cm^{-1} in AOT and BHDC RMs, respectively. These important variations in the $\Delta\nu_{asym}SO_3$ values with the W_s suggest that the TfO's asymmetric sulfonate stretching in bmimTfO entrapped in RMs is particularly modified by the presence of different ions at the interface. Thus, the observation of a $\Delta\nu_{asym}SO_3$ value in both RMs suggests a stronger cation–TfO interaction than the weak $bmim^+$–TfO^- interaction observed in neat IL. Thus, the presence of other cations different to $bmim^+$ near the TfO^- environment could be the main reason for the $\Delta\nu_{asym}SO_3$ values observed, especially at low W_s. In this sense, at the interface of AOT RMs the counterion Na^+ could replace with the $bmim^+$ in the TfO^- vicinity forming a new ion pair: Na^+–TfO^-. A similar situation could occur in the BHDC RMs, but in this organized system the positive charge of the BHDC head group (BHD^+) is now near the TfO^- anion at the interface producing the ion pair: BHD^+–TfO^-. The differences in the $\Delta\nu_{asym}SO_3$ magnitude observed between AOT and BHDC RMs can be assigned to the size and nature of the cations involved in the interaction, however in both cases the replacement of $bmim^+$ for Na^+ or BHD^+ affects the asymmetric sulfonate stretching of TfO^- producing a splitting in the band. Segregation of these ions decreases with the amount of IL entrapped, however even at the maximum W_s reached the $\Delta\nu_{asym}SO_3$ values are not zero as in the neat bmimTfO.

Thus, as it was explained for the C(4,5)–H vibration mode, the $\Delta\nu_{asym}SO_3$ showed in Fig. 5 can be interpreted as a consequence of an electrostatic interaction between the positive charge of the BHDC head group (BHD^+) or the counterion Na^+ of AOT and the anion TfO^-. This interaction can affect considerably the bmimTfO structure when it is encapsulated in RMs. As the positive charge is located exclusively in the quaternary nitrogen atom of BHD^+ or in the small Na^+ while the positive charge is delocalized in the $bmim^+$ ion (see Scheme 1),[94] we expect a stronger interaction between TfO^-

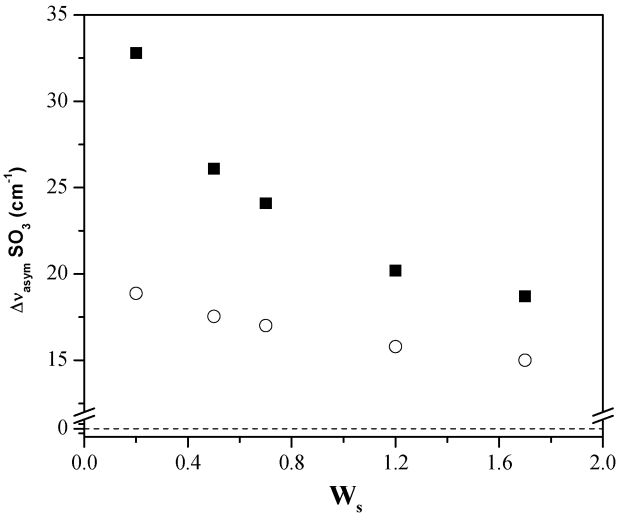

Fig. 5 Splitting of the TfO's asymmetric S═O stretching band frequency ($\Delta\nu_{asym}SO_3$) upon increasing W_s in different chlorobenzene/surfactant/bmimTfO RMs. AOT (■) and BHDC (○). [Surfactant] = 0.02 M. The corresponding value for neat bmimTfO (---) is included for comparison.

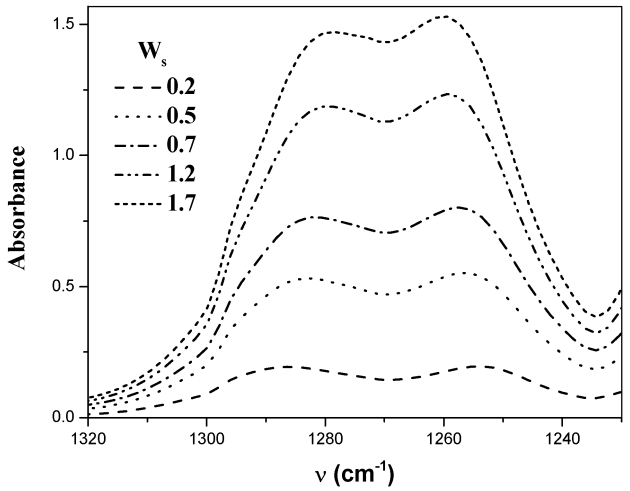

Fig. 4 FT-IR spectra of bmimTfO entrapped in chlorobenzene/AOT RMs at different W_s values, in the region of 1320–1230 cm^{-1}. [AOT] = 0.02 M. The chlorobenzene and AOT bands have been subtracted.

and the BHD^+ head group or Na^+ than with its own $bmim^+$ cations forming probably ion pairing. The large $\Delta\nu_{asym}SO_3$ value obtained at low W_s in the AOT and BHDC RMs shown in Fig. 5 agrees with a strong electrostatic interaction between TfO^- and Na^+ or BHD^+, respectively.

In conclusion, effects in both the cation (Fig. 3A) and the anion (Fig. 5) of the bmimTfO when combined with the cationic or anionic surfactant are observed. In consequence, all the results observed (DLS and FT-IR) for bmimTfO entrapped in AOT or BHDC RMs show strong IL–surfactant interaction and significant changes in structural organization of the interface of RMs. Thus, we assume that the ion pair degree in bmimTfO must be altered when it is encapsulated inside the both RMs, especially at low IL content, producing an interface more electron donor than the bmimTfO neat. The ILs distribution at the interface in the AOT and BHDC RMs can be represented as in the Scheme 2A. Layering (or segregation) of ILs has been observed in homogeneous systems[95] and especially in similar RMs,[26–28] showing the versatility of this kind of organized systems to alter the ionic organization.

(2.3) TfA's asymmetric carboxylate stretching band ($\nu_{asym}COO^-$). TfA^- is an anion where the carbonyl groups are indistinguishable because the negative charge is delocalized over both oxygens.[72] Consequently, there are two absorption bands, one from an asymmetrically coupled vibration and the other from a symmetrically coupled stretching. Both absorptions are found at lower frequency than an isolated (ketone) C═O function.[72] Thus, in the lower wavenumber region, the band at around 1600 cm^{-1} results from the asymmetric stretching vibration of COO^- and its symmetric stretching mode lies in the range of 1300–1450 cm^{-1}.[96,97] The asymmetric mode has a strong IR activity whereas the symmetric mode is less active.[97] This asymmetric stretching vibrations in TfA^- can play a relevant role in order to evaluate the cation–TfA interactions.[98,99] In this sense, the FT-IR behavior of different TfA metallic salts was studied in the past and the interpretation of data was quite complex because TfA^- can act as a monodentate, bidentate and/or bridging ligand depending on the nature (size and charge) of the cation involved.[98,100] For example, the $\nu_{asym}COO^-$ value for NaTfA appears at 1680 cm^{-1} whereas in NH_4TfA the frequency is 1667 cm^{-1} acting in both cases as monodentate ligands. However, the ν_aCOO^- stretching frequencies for the purely bridging TfA^- are observed at higher wavenumbers than those concerned with either chelating or both bridging and chelating TfA^-.[101]

BmimTfA, which is an IL whose anion has very high electron donor ability[46,102] present a strong and almost symmetric band at 1689 cm^{-1}, which is attributed to asymmetric carboxylate stretching vibration.[103–105] The interaction of bmimTfA with solvents was studied in the past and the results showed that also affects this vibration mode.[102,105] For example, the $\nu_{asym}COO^-$ values showed shifts to low wavenumbers upon addition of water (or methanol) to pure bmimTfA,[102,105] which represent the weakening of the C═O bond. Moreover, considering the

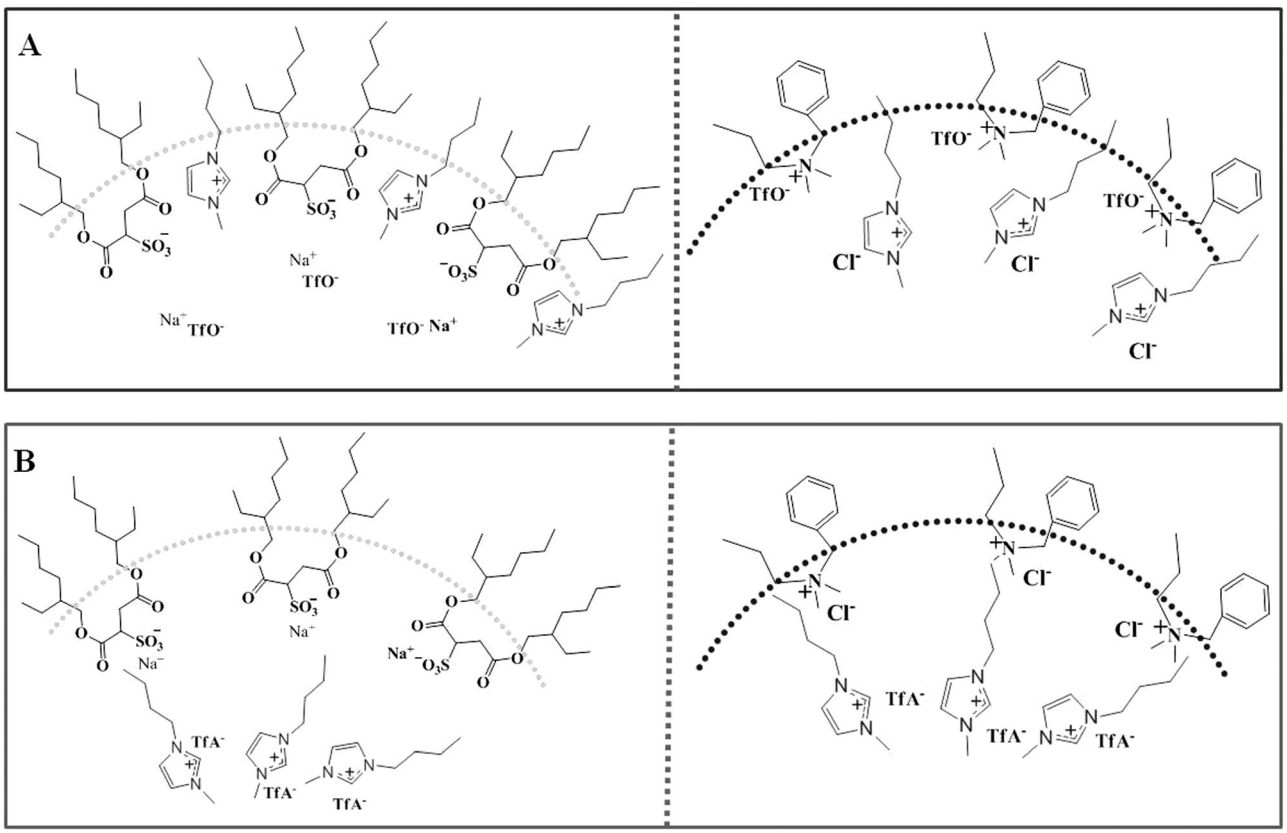

Scheme 2 Schematic representation of the ILs distribution in the AOT and BHDC RMs: (A) bmimTfO and (B) bmimTfA.

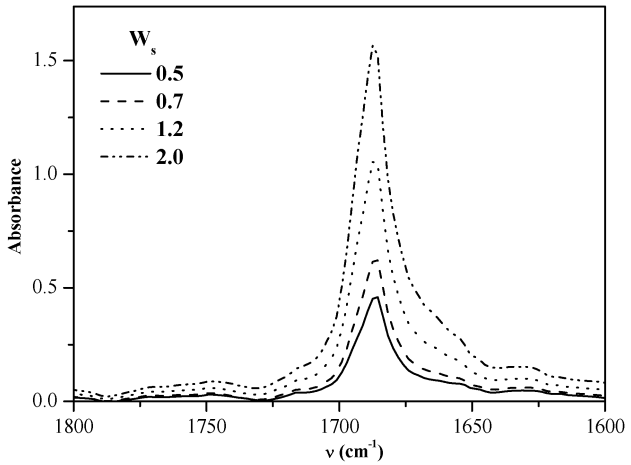

Fig. 6 FT-IR spectra of bmimTfA entrapped in chlorobenzene/BHDC RMs at different W_s values, in the region of 1800–1600 cm^{-1} (TfA's $\nu_{asym}COO^-$). The chlorobenzene bands have been subtracted. [BHDC] = 0.02 M.

general understanding that carboxylate group is a good proton acceptor, the shifting was explained considering H-bonding interaction between water and TfA^-.[105] Thus, the interaction of water with bmimTfA shows direct evidence that water molecules are bound to the COO^- end of the anion.[102]

Typical FT-IR spectra of bmimTfA inside chlorobenzene/BHDC RMs at different W_s values, in the region of 1800–1600 cm^{-1} corresponding to the asymmetric carboxylate stretching frequency of TfA^-, are shown in Fig. 6. FT-IR spectra obtained for chlorobenzene/AOT/bmimTfA RMs are presented in Fig. S4 (ESI†). Shifts of the TfA's $\nu_{asym}COO^-$ values upon increase of W_s in both RMs studied are shown in Fig. 7. As it can be observed, all the asymmetric carboxylate stretching frequency values in RMs are very similar in both RMs studied and slightly lower than that corresponding to neat bmimTfA (1689 cm^{-1}). Additionally, Fig. 7 also shows that the $\nu_{asym}COO^-$ values for bmimTfA in AOT or BHDC RMs are practically constant, around 1687 cm^{-1}, in the whole W_s range studied. The absence of variations in the $\nu_{asym}COO^-$ values with W_s and the similitude with the neat value show that the TfA's asymmetric carboxylate stretching in bmimTfA entrapped in RMs is not modified by the interface. However, the slightly lower $\nu_{asym}COO^-$ values than that obtained for neat bmimTfA suggest a relatively stronger TfA^-–$bmim^+$ interaction in both RMs than in bulk IL.

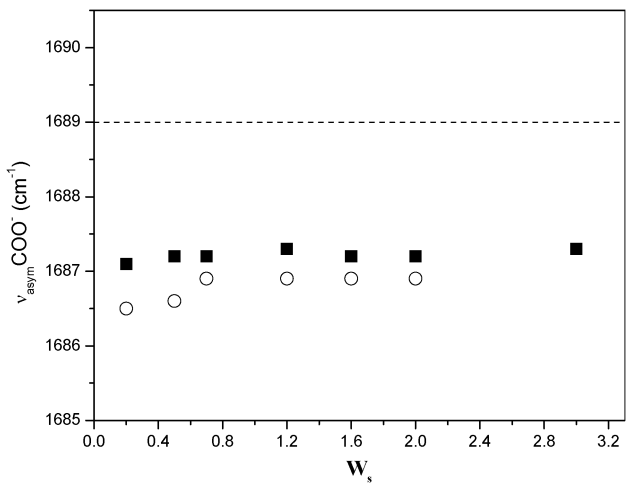

Fig. 7 Shift of the TfA's asymmetric carboxylate stretching frequency ($\nu_{asym}COO^-$) upon increase of W_s in different chlorobenzene/surfactant/bmimTfA RMs. AOT (■) and BHDC (○). [Surfactant] = 0.02 M. The corresponding value for neat bmimTfA (---) is included for comparison.

The results found entrapping bmimTfA in AOT or BHDC RMs, especially the vibration modes observed (Fig. 3B and 7), clearly show a different situation in comparison with the results of bmimTfO. The data of bmimTfA obtained following the behavior of $bmim^+$ in both RMs (Fig. 3B) show that the values of ν_{C-H} are lower than the neat bmimTfA, suggesting again a decrease in the positive charge of the cation. However, the absence of changes with W_s and the kind of interface used to generate RMs suggest that $bmim^+$ interacts more strongly with TfA^- than with the surfactants. If we analyze the results following the TfA's behavior in both RMs (Fig. 7), it is possible to think that the lower $\nu_{asym}COO^-$ values than that obtained for neat bmimTfA show the weakening of the C═O bond, due to a strong cation interaction. We suggest that this behavior again is a consequence of a stronger interaction between TfA^-–$bmim^+$ than in bulk IL. Thus, we think that the small changes observed by FT-IR in the AOT and BHDC RMs varying the IL content and the type of interface are evidence of a weak interaction between the surfactants and bmimTfA, and as it was showed also by DLS suggesting that there is little (if any) penetration of bmimTfA at the interface. Considering all the results reported here, the interfacial zone in these RMs can be represented as in Scheme 2B. Finally, it is important to note that in any case (AOT or BHDC) even at the maximum value of W_s reached the behavior of bmimTfA confined in both RMs is not equal to the characteristics observed for the neat bmimTfA. These results suggest that even that the IL–surfactant interaction is weak, the ion pairing effect between $bmim^+$–TfA^- is substantially enhanced upon confinement, altered the structure and properties of the entrapped bmimTfA. For example, we anticipate a decrease in the electron donor ability of the RM interfaces in comparison with the bmimTfA neat.

Conclusions

In summary, we have shown the existence of different chlorobenzene/surfactant/IL RMs and that the IL structures sequestrated depend strongly on the type of surfactant used to create the RMs. DLS results reveal the formation of RMs containing bmimTfO and bmimTfA as polar components since the droplet size values increase as the W_s values increase. Furthermore, it shows that the RMs consist of discrete spherical and non-interacting droplets of IL stabilized by the surfactants. The large droplets size values and the larger changes observed for bmimTfO entrapped in AOT and BHDC RMs in comparison with the values obtained for bmimTfA in both RMs can be explained considering the different IL–surfactant interactions.

The types of interactions involved are deduced using FT-IR spectroscopy. The FT-IR results suggest that the ionic interactions (with the surfactant polar head groups, surfactant counterions or with the IL counterions) are substantially modified upon confinement. These interactions produce segregation of IL's ions, altering the composition of the RM interfaces in the case of bmimTfO or more ion pairing in the bmimTfA case. These facts show the versatility of this kind of organized systems to alter the ionic organization, information that can be very important if these media are used as nanoreactors because unique microenvironments can be easily created simply changing the RM components and W_s.

Acknowledgements

We gratefully acknowledge the financial support for this work by the Consejo Nacional de Investigaciones Científicas y Técnicas (CONICET), Agencia Nacional de Promoción Científica y Técnica, Agencia Córdoba Ciencia and Secretaría de Ciencia y Técnica de la Universidad Nacional de Río Cuarto. N.M.C., J.J.S. and R.D.F. hold a research position at CONICET. D.B. thanks CONICET for a research fellowship.

References

1 T. K. De and A. Maitra, *Adv. Colloid Interface Sci.*, 1995, **59**, 95.
2 J. J. Silber, M. A. Biasutti, E. Abuin and E. Lissi, *Adv. Colloid Interface Sci.*, 1999, **82**, 189.
3 S. P. Moulik and B. K. Paul, *Adv. Colloid Interface Sci.*, 1998, **78**, 99.
4 N. M. Correa, M. A. Biasutti and J. J. Silber, *J. Colloid Interface Sci.*, 1995, **172**, 71.
5 N. M. Correa, M. A. Biasutti and J. J. Silber, *J. Colloid Interface Sci.*, 1996, **184**, 570.
6 N. M. Correa, R. D. Falcone, M. A. Biasutti and J. J. Silber, *Langmuir*, 2000, **16**, 3070.
7 R. McNeil and J. K. Thomas, *J. Colloid Interface Sci.*, 1981, **83**, 57.
8 A. M. Durantini, R. D. Falcone, J. J. Silber and N. M. Correa, *ChemPhysChem*, 2009, **10**, 2034.
9 R. D. Falcone, J. J. Silber and N. M. Correa, *Phys. Chem. Chem. Phys.*, 2009, **11**, 11096.
10 F. Moyano, S. S. Quintana, R. D. Falcone, J. J. Silber and N. M. Correa, *J. Phys. Chem. B*, 2009, **113**, 4284.
11 A. Jada, J. Lang, R. Zana, R. Makhloufi, E. Hirsch and S. J. Candau, *J. Phys. Chem.*, 1990, **94**, 381.
12 M. S. Baptista and C. D. Tran, *J. Phys. Chem. B*, 1997, **101**, 4209.
13 D. Grand, *J. Phys. Chem. B*, 1998, **102**, 4322.
14 S. S. Quintana, F. Moyano, R. D. Falcone, J. J. Silber and N. M. Correa, *J. Phys. Chem. B*, 2009, **113**, 6718.
15 F. Moyano, R. D. Falcone, J. C. Mejuto, J. J. Silber and N. M. Correa, *Chem.–Eur. J.*, 2010, **16**, 8887.
16 A. M. Durantini, R. D. Falcone, J. J. Silber and N. M. Correa, *J. Phys. Chem. B*, 2011, **115**, 5894.
17 D. Blach, N. M. Correa, J. J. Silber and R. D. Falcone, *J. Colloid Interface Sci.*, 2011, **355**, 124.
18 F. M. Agazzi, R. D. Falcone, J. J. Silber and N. M. Correa, *J. Phys. Chem. B*, 2011, **115**, 12076.
19 F. O. Silva, M. A. Fernández, J. J. Silber, R. H. De Rossi and N. M. Correa, *ChemPhysChem*, 2012, **13**, 124.
20 D. Grand and A. Dokutchaev, *J. Phys. Chem. B*, 1997, **101**, 3181.
21 S. M. B. Costa and R. L. Brookfield, *J. Chem. Soc., Faraday Trans. 2*, 1986, **82**, 991.
22 J. A. Gutierrez, R. D. Falcone, J. J. Silber and N. M. Correa, *Dyes Pigm.*, 2012, **95**, 290.
23 N. M. Correa and N. E. Levinger, *J. Phys. Chem. B*, 2006, **110**, 13050.
24 M. Novaira, F. Moyano, M. A. Biasutti, J. J. Silber and N. M. Correa, *Langmuir*, 2008, **24**, 4637.
25 S. S. Quintana, R. D. Falcone, J. J. Silber and N. M. Correa, *ChemPhysChem*, 2012, **13**, 115.
26 R. D. Falcone, N. M. Correa and J. J. Silber, *Langmuir*, 2009, **25**, 10426.
27 R. D. Falcone, B. Baruah, E. Gaidamauskas, C. D. Rithner, N. M. Correa, J. J. Silber, D. C. Crans and N. E. Levinger, *Chem.–Eur. J.*, 2011, **17**, 6837.
28 D. D. Ferreyra, N. M. Correa, J. J. Silber and R. D. Falcone, *Phys. Chem. Chem. Phys.*, 2012, **14**, 3460.
29 N. M. Correa, J. J. Silber, R. E. Riter and N. E. Levinger, *Chem. Rev.*, 2012, **112**, 4569.
30 (*a*) T. Welton, *Green Chem.*, 2011, **13**, 225; (*b*) J. P. Hallett and T. Welton, *Chem. Rev.*, 2011, **111**, 3508; (*c*) P. Wasserscheid and W. Keim, *Angew. Chem., Int. Ed.*, 2000, **39**, 3772; (*d*) T. Welton, *Chem. Rev.*, 1999, **99**, 2071.
31 T. Welton and P. Wasserscheid, *Ionic Liquids in Synthesis*, VCH-Wiley, Weinheim, 2002.
32 T. Welton, *Coord. Chem. Rev.*, 2004, **248**, 2459.
33 L. Crowhurst, R. Falcone, N. L. Lancaster, V. Llopis-Mestre and T. Welton, *J. Org. Chem.*, 2006, **71**, 8847.
34 (*a*) D. K. Sasmal, S. S. Mojumdar, A. Adhikari and K. Bhattacharyya, *J. Phys. Chem. B*, 2010, **114**, 4565; (*b*) R. Pramanik, S. Sarkar, C. Ghatak, P. Setua, V. G. Rao and N. Sarkar, *Chem. Phys. Lett.*, 2010, **490**, 154; (*c*) S. S. Mojumdar, T. Mondal, A. K. Das, S. Dey and K. Bhattacharyya, *J. Chem. Phys.*, 2010, **132**, 194505; (*d*) M. Moniruzzaman, N. Kamiya and M. Goto, *J. Colloid Interface Sci.*, 2010, **352**, 136; (*e*) S. Debnath, D. Das, S. Dutta and P. K. Das, *Langmuir*, 2010, **26**, 4080.
35 J. Hao and T. Zemb, *Curr. Opin. Colloid Interface Sci.*, 2007, **12**, 129.
36 (*a*) D. Chakrabarty, D. Seth, A. Chakraborty and N. Sarkar, *J. Phys. Chem. B*, 2005, **109**, 5753; (*b*) H. X. Gao, J. C. Li, B. X. Han, W. N. Chen, J. L. Zhang, R. Zhang and D. D. Yan, *Phys. Chem. Chem. Phys.*, 2004, **6**, 2914; (*c*) Y. Gao, N. Li, L. Q. Zheng, X. T. Bai, L. Yu, X. Y. Zhao, J. Zhang, M. W. Zhao and Z. Li, *J. Phys. Chem. B*, 2007, **111**, 2506; (*d*) Y. Gao, J. Zhang, H. Y. Xu, X. Y. Zhao, L. Q. Zheng, X. W. Li and L. Yu, *ChemPhysChem*, 2006, **7**, 1554; (*e*) Y. N. Gao, S. B. Han, B. X. Han, G. Z. Li, D. Shen,

Z. H. Li, J. M. Du, W. G. Hou and G. Y. Zhang, *Langmuir*, 2005, **21**, 5681; (*f*) T. L. Merrigan, E. D. Bates, S. C. Dorman and J. H. Davis, *Chem. Commun.*, 2000, 2051; (*g*) G. M. Sando, K. Dahl and J. C. Owrutsky, *Chem. Phys. Lett.*, 2006, **418**, 402; (*h*) F. Yan and J. Texter, *Chem. Commun.*, 2006, 2696.

37 (*a*) N. Li, Q. Cao, Y. A. Gao, J. Zhang, L. Q. Zheng, X. T. Bai, B. Dong, Z. Li, M. W. Zhao and L. Yu, *ChemPhysChem*, 2007, **8**, 2211; (*b*) A. Chakraborty, D. Seth, D. Chakrabarty, P. Setua and N. Sarkar, *J. Phys. Chem. A*, 2005, **109**, 11110; (*c*) J. Eastoe, S. Gold, S. E. Rogers, A. Paul, T. Welton, R. K. Heenan and I. Grillo, *J. Am. Chem. Soc.*, 2005, **127**, 7302; (*d*) N. Li, Y. A. Gao, L. Q. Zheng, J. Zhang, L. Yu and X. W. Li, *Langmuir*, 2007, **23**, 1091; (*e*) J. H. Liu, S. Q. Cheng, J. L. Zhang, X. Y. Feng, X. G. Fu and B. X. Han, *Angew. Chem., Int. Ed.*, 2007, **46**, 3313.

38 F. Gayet, C. El Kalamouni, P. Lavedan, J.-D. Marty, A. Brulet and N. Lauth-de Viguerie, *Langmuir*, 2009, **25**, 9741.

39 Y. Zheng, W. Eli and G. Li, *Colloid Polym. Sci.*, 2009, **287**, 871.

40 (*a*) A. Adhikari, K. Sahu, S. Dey, S. Ghosh, U. Mandal and K. Bhattacharyya, *J. Phys. Chem. B*, 2007, **111**, 12809; (*b*) K. A. Fletcher and S. Pandey, *Langmuir*, 2004, **20**, 33; (*c*) J. C. Li, J. L. Zhang, H. X. Gao, B. X. Han and L. Gao, *Colloid Polym. Sci.*, 2005, **283**, 1371; (*d*) J. C. Li, J. L. Zhang, B. X. Han, Y. Wang and L. Gao, *J. Chem. Phys.*, 2004, **121**, 7408.

41 (*a*) O. Rojas, J. Koetz, S. Kosmella, B. Tiersch, P. Wacker and M. Kramer, *J. Colloid Interface Sci.*, 2009, **333**, 782; (*b*) C. Rabe and J. Koetz, *Colloids Surf., A*, 2010, **354**, 261.

42 (*a*) R. Pramanik, S. Sarkar, C. Ghatak, V. G. Rao and N. Sarkar, *Chem. Phys. Lett.*, 2011, **512**, 217; (*b*) R. Pramanik, C. Ghatak, V. G. Rao, S. Sarkar and N. Sarkar, *J. Phys. Chem. B*, 2011, **115**, 5971.

43 M. Andujar-Matalobos, L. Garcia-Rio, S. Lopez-Garcia and P. Rodriguez-Dafonte, *J. Colloid Interface Sci.*, 2011, **363**, 261.

44 S. Cheng, J. Zhang, Z. Zhang and B. Han, *Chem. Commun.*, 2007, 2497.

45 (*a*) M. Moniruzzaman, N. Kamiya, K. Nakashima and M. Goto, *ChemPhysChem*, 2008, **9**, 689; (*b*) M. Moniruzzaman, N. Kamiya, K. Nakashima and M. Goto, *Green Chem.*, 2008, **10**, 497.

46 (*a*) R. Lungwitz, M. Friedrich, W. Linert and S. Spange, *New J. Chem.*, 2008, **32**, 1493; (*b*) R. Lungwitz and S. Spange, *New J. Chem.*, 2008, **32**, 392.

47 (*a*) G. Ranieri, J. P. Hallett and T. Welton, *Ind. Eng. Chem. Res.*, 2008, **47**, 638; (*b*) J. P. Hallett, C. L. Liotta, G. Ranieri and T. Welton, *J. Org. Chem.*, 2009, **74**, 1864.

48 R. E. Riter, J. R. Kimmel, E. P. Undiks and N. E. Levinger, *J. Phys. Chem. B*, 1997, **101**, 8292.

49 L. P. Novaki, N. M. Correa, J. J. Silber and O. A. El Seoud, *Langmuir*, 2000, **16**, 5573.

50 N. M. Correa, P. A. R. Pires, J. J. Silber and O. A. El Seoud, *J. Phys. Chem. B*, 2005, **109**, 21209.

51 A. Salabat, J. Eastoe, K. J. Mutch and F. Tabor Rico, *J. Colloid Interface Sci.*, 2008, **318**, 244.

52 M. L. Stahla, B. Baruah, D. M. James, M. D. Johnson, N. E. Levinger and D. C. Crans, *Langmuir*, 2008, **24**, 6027.

53 (*a*) F. Heatley, *J. Chem. Soc., Faraday Trans. 1*, 1989, **85**, 917; (*b*) F. Heatley, *J. Chem. Soc., Faraday Trans. 1*, 1988, **84**, 343; (*c*) F. Heatley, *J. Chem. Soc., Faraday Trans. 1*, 1987, **83**, 517.

54 O. A. El Seoud, N. M. Correa and L. P. Novaki, *Langmuir*, 2001, **17**, 1847.

55 J. Dupont, P. A. Z. Suarez, C. S. Consorti and R. F. de Souza, *Org. Synth.*, 2002, **79**, 236.

56 P. Bonhôte, A.-P. Dias, M. Armand, N. Papageorgiou, K. Kalyanasundaram and M. Grätzel, *Inorg. Chem.*, 1998, **37**, 166.

57 P. Nockemann, K. Binnemans and K. Driesen, *Chem. Phys. Lett.*, 2005, **415**, 131.

58 P. Brown, C. P. Butts, J. Eastoe, D. Fermin, I. Grillo, H.-C. Lee, D. Parker, D. Plana and R. M. Richardson, *Langmuir*, 2012, **28**, 2502.

59 M. A. Sedgwick, A. M. Trujillo, N. Hendricks, N. E. Levinger and D. C. Crans, *Langmuir*, 2011, **27**, 948.

60 (*a*) J. P. Blitz, J. L. Fulton and R. D. Smith, *J. Phys. Chem.*, 1988, **92**, 2707; (*b*) H. B. Bohidar and M. Behboudina, *Colloids Surf., A*, 2001, **178**, 313.

61 C. A. Gracia, S. Gomez-Barreiro, A. Gonzalez-Perez, J. Nimo and J. R. Rodriguez, *J. Colloid Interface Sci.*, 2004, **276**, 408.

62 P. D. Moran, A. Graham, A. Bowmaker, R. P. Cooney, J. R. Barlett and J. L. Woolfrey, *Langmuir*, 1995, **11**, 738.

63 P. D. Moran, G. A. Bowmaker, R. P. Cooney, J. R. Bartlettb and J. L. Woolfrey, *J. Mater. Chem.*, 1995, **5**, 295.

64 A. Salabat, J. Eastoe, K. J. Mutch and F. Tabor Rico, *J. Colloid Interface Sci.*, 2008, **318**, 244.

65 A. Maitra, *J. Phys. Chem.*, 1984, **88**, 5122.

66 Q. Li, T. Li and J. Wu, *J. Colloid Interface Sci.*, 2001, **239**, 522.

67 C. Reichardt, *Green Chem.*, 2005, **7**, 339.

68 N. Gorski and Y. M. Ostanevich, *Ber. Bunsen-Ges. Phys. Chem.*, 1990, **94**, 737.

69 A. Jada, J. Lang, R. Zana, R. Makhloufi, E. Hirsch and S. J. Candau, *J. Phys. Chem.*, 1990, **94**, 387.

70 J. C. Lassegues, J. Grondin, D. Cavagnat and P. Johansson, *J. Phys. Chem. A*, 2009, **113**, 6419.

71 (*a*) J. Shi, P. Wu and F. Yan, *Langmuir*, 2010, **26**, 11427; (*b*) Q.-G. Zhang, N.-N. Wang and Z.-W. Yu, *J. Phys. Chem. B*, 2010, **114**, 4747; (*c*) K. Noack, P. S. Schulz, N. Paape, J. Kiefer, P. Wasserscheid and A. Leipertz, *Phys. Chem. Chem. Phys.*, 2010, **12**, 14153.

72 R. M. Silverstein, F. X. Webster and D. J. Kiemle, *Spectrometric Identification of Organic Compounds*, J. Wiley, New York, 7th edn, 2005.

73 S. A. Suthanthiraraj, R. Kumar and B. J. Paul, *Ionics*, 2010, **16**, 145.

74 D. H. Johnston and D. F. Shriver, *Inorg. Chem.*, 1993, **32**, 1045.

75 J. M. Alía, Y. Díaz de Mera, H. G. M. Edwards, F. J. García and E. E. Lawson, *J. Mol. Struct.*, 1997, **408**, 439.

76 J. M. Alía and H. G. M. Edwards, *Vib. Spectrosc.*, 2000, **24**, 185.

77 A. Bernson and J. Lindgren, *Polymer*, 1994, **35**, 4842.
78 J.-M. Andanson, F. Jutz and A. Baiker, *J. Supercrit. Fluids*, 2010, **55**, 395.
79 A. Wendsjö, J. Lindgren, J. O. Thomas and G. C. Farrington, *Solid State Ionics*, 1992, **53**, 1077.
80 A. Bernson and J. Lindgren, *Solid State Ionics*, 1993, **60**, 37.
81 A. Bernson and J. Lindgren, *Solid State Ionics*, 1993, **60**, 31.
82 P.-A. Bergström and R. Frech, *J. Phys. Chem.*, 1995, **99**, 12603.
83 A. G. Bishop, D. R. MacFarlane, D. McNaughton and M. Forsyth, *J. Phys. Chem.*, 1996, **100**, 2237.
84 A. Bernson, J. Lindgren, W. Huang and R. Frech, *Polymer*, 1995, **36**, 4471.
85 M. C. Goncalves, V. de Zea Bermudez, D. Ostrovskii and L. D. Carlos, *Solid State Ionics*, 2004, **166**, 103.
86 C. M. Burba, N. M. Rocher and R. Frech, *J. Phys. Chem. B*, 2009, **113**, 11453.
87 W. Huang and R. Frech, *Polymer*, 1994, **35**, 235.
88 R. Frech, S. Chintapalli, P. G. Bruce and C. A. Vincent, *Macromolecules*, 1999, **32**, 808.
89 A. Bakker, J. Lindgren and K. Hermansson, *Polymer*, 1996, **37**, 1871.
90 S. P. Gejji, K. Hermansson, J. Tegenfeldt and J. Lindgren, *J. Phys. Chem.*, 1993, **97**, 11402.
91 R. Frech and W. Huang, *J. Solution Chem.*, 1994, **23**, 469.
92 E. Kamienska-Piotrowicz, J. Stangret and J. Szymanska-Cybulska, *Spectrochim. Acta, Part A*, 2007, **66**, 1.
93 T. Iwahashi, T. Miyamae, K. Kanai, K. Seki, D. Kim and Y. Ouchi, *J. Phys. Chem. B*, 2008, **112**, 11936.
94 D. R. McFarlane, J. Sun, J. Golding, P. Meakin and M. Forsyth, *Electrochim. Acta*, 2000, **45**, 1271.
95 (*a*) B. L. Bhargava, R. Devane, M. L. Klein and S. Balasubramanian, *Soft Matter*, 2007, **3**, 1395; (*b*) O. Russina, L. Gontrani, B. Fazio, D. Lombardo, A. Triolo and R. Caminiti, *Chem. Phys. Lett.*, 2010, **493**, 259; (*c*) K. Iwata, H. Okajima, S. Saha and H. Hamaguchi, *Acc. Chem. Res.*, 2007, **40**, 1174; (*d*) D. A. Turton, J. Hunger, A. Stoppa, G. Hefter, A. Thoman, M. Walther, R. Buchner and K. Wynne, *J. Am. Chem. Soc.*, 2009, **131**, 11140; (*e*) A. Triolo, O. Russina, H.-J. Bleif and E. Di Cola, *J. Phys. Chem. B*, 2007, **111**, 4641; (*f*) J. N. A. Canongia Lopes and A. A. H. Padua, *J. Phys. Chem. B*, 2006, **110**, 3330; (*g*) Q. Kuang, J. Zhang and Z. Wang, *J. Phys. Chem. B*, 2007, **111**, 9858; (*h*) J. de Andrade, E. S. Böes and H. Stassen, *J. Phys. Chem. B*, 2008, **112**, 8966; (*i*) Y. Wang and G. A. Voth, *J. Am. Chem. Soc.*, 2005, **127**, 12192.
96 Z. H. Sun, W. M. Sun, C. T. Chen, G. H. Zhang, X. Q. Wang and D. Xu, *Spectrochim. Acta, Part A*, 2011, **83**, 39.
97 M. I. Cabaco, M. Besnard, Y. Danten and J. A. P. Coutinho, *J. Phys. Chem. B*, 2011, **115**, 3538.
98 G. B. Deacon and R. J. Phillips, *Coord. Chem. Rev.*, 1980, **33**, 227.
99 P.-A. Bergström and J. Lindgren, *J. Mol. Struct.*, 1991, **245**, 221.
100 S. Mishra, G. Ledoux, E. Jeanneau, S. Daniele and M.-F. Joubert, *Dalton Trans.*, 2012, **41**, 1490.
101 S. Mishra, J. Zhang, L. G. Hubert-Pfalzgraf, D. Luneau and E. Jeanneau, *Eur. J. Inorg. Chem.*, 2007, 602.
102 L. Cammarata, S. G. Kazarian, P. A. Salter and T. Welton, *Phys. Chem. Chem. Phys.*, 2001, **3**, 5192.
103 A. A. Strechan, Y. U. Paulechka, A. V. Blokhin and G. J. Kabo, *J. Chem. Thermodyn.*, 2008, **40**, 632.
104 A. Podgorsek, M. Macchiagodena, F. Ramondo, M. F. Costa Gomes and A. A. H. Pádua, *ChemPhysChem*, 2012, **13**, 1753.
105 Q.-G. Zhang, N.-N. Wang, S.-L. Wang and Z.-W. Yu, *J. Phys. Chem. B*, 2011, **115**, 11127.